An interpolating reproducing kernel particle method for two-dimensional scatter points*

Qin Yi-Xiao(秦义校)[a)†], Liu Ying-Ying(刘营营)[a)], Li Zhong-Hua(李中华)[a)b)], and Yang Ming(杨 明)[a)]

[a)] College of Mechanical Engineering, Taiyuan University of Science and Technology, Taiyuan 030024, China
[b)] Shantui Construction Machinery Co., Ltd, Jining 272000, China

(Received 26 November 2013; revised manuscript received 22 January 2014; published online 15 May 2014)

An interpolating reproducing kernel particle method for two-dimensional (2D) scatter points is introduced. It eliminates the dependency of gridding in numerical calculations. The interpolating shape function in the interpolating reproducing kernel particle method satisfies the property of the Kronecker delta function. This method offers a mathematics basis for recognition technology and simulation analysis, which can be expressed as simultaneous differential equations in science or project problems. Mathematical examples are given to show the validity of the interpolating reproducing kernel particle method.

Keywords: interpolating reproducing kernel particle method, point interpolating characteristic, scatter points

PACS: 02.60.–x, 02.60.Cb, 46.25.–y **DOI:** 10.1088/1674-1056/23/7/070207

1. Introduction

In recent years, many meshless methods have been developed, such as the element-free Galerkin (EFG) method,[1–3] the diffuse element method, the meshless local Petrov-Galerkin method (MLPG), the meshless point collocation method (PCM),[4] the complex variable meshless method,[5–13] and the meshless boundary integral equation methods.[14–19]

The interpolating reproducing kernel particle method (IRKPM) is one of the meshless methods. In 1996, Liu used the wavelet analysis characteristics such as scale expansion translation and multi-resolution to present the multiple-scale reproducing kernel particle method and the wavelet particle method, and these methods realized the adaptive analysis.[20] In 1997, Li and Liu presented the moving least-square reproducing kernel particle method.[21] In 2000, Chen and some other scholars improved the reproducing kernel particle method, and applied it to the incompressible limited elastomer analysis.[22] Domestic scholars also researched the RKPM and its practical application. Cheng and Peng presented a direct meshless boundary integral equation method, called the boundary element-free method, to solve two-dimensional linear elastodynamic problems.[23] Based on the element-free Galerkin (EFG) method and the improved complex variable moving least-square (ICVMLS) approximation, Cheng and Wang presented the improved complex variable element-free Galerkin (ICVEFG) method to solve two-dimensional problems and transient heat conduction problems.[24–26] The RKPM not only shares the common features of all meshless methods but also has some unique features, such as time or space localisation, hp-like adaptivity, as well as multi-resolution analysis. The interpolating RKPM is an interesting numerical technique that can solve many engineering problems as mechanical and potential problems. It is evident that the numerical results of the interpolating RKPM are in excellent agreement with the analytical solution, and the validity and availability by numerical arithmetic analyses are verified.

2. The IRKPM for two-dimensional approximation

For a given point $\boldsymbol{x}(x_1,x_2)\in\Omega$, define the approximation function $u(\boldsymbol{x})\approx u^{\mathrm{h}}(\boldsymbol{x})=\sum\Psi_I(\boldsymbol{x})u_I$, and the shape function in the interpolating RKPM can be expressed as

$$\Psi_I(\boldsymbol{x})=\hat{\Psi}_I(\boldsymbol{x})+\bar{\Psi}_I(\boldsymbol{x}). \tag{1}$$

Here $\hat{\Psi}_I(\boldsymbol{x})$ can be formed by the weight function $\hat{\Phi}_{\hat{a}_I}(\boldsymbol{x}-\boldsymbol{x}_I)$ of particle $\boldsymbol{x}_I$ and its value

$$\hat{\Psi}_I(\boldsymbol{x})=\frac{\hat{\Phi}_{\hat{a}_I}(\boldsymbol{x}-\boldsymbol{x}_I)}{\hat{\Phi}_{\hat{a}_I}(0)},$$
$$\hat{a}_I<\min\{\|\boldsymbol{x}_I-\boldsymbol{x}_J\|\ \forall J\neq I\}. \tag{2}$$

It satisfies the property of the Kronecker delta function. The $\bar{\Psi}_I(\boldsymbol{x})$ is formed by extending the reproducing condition, and the concrete form is

$$\hat{\Psi}_I(\boldsymbol{x})=\boldsymbol{H}^{\mathrm{T}}(\boldsymbol{x}-\boldsymbol{x}_I)\boldsymbol{Q}^{-1}(\boldsymbol{x})[\boldsymbol{H}(\boldsymbol{0})-\hat{\boldsymbol{H}}(\boldsymbol{x})]\bar{\Phi}_{\hat{a}_I}(\boldsymbol{x}-\boldsymbol{x}_I), \tag{3}$$

here $\boldsymbol{H}(\boldsymbol{x}-\boldsymbol{x}_I)$ is the basis function vector

$$\boldsymbol{H}^{\mathrm{T}}(\boldsymbol{x}-\boldsymbol{x}_I)=[1\ \ x_1-x_{I1}\ \ x_2-x_{I2}\ \ (x_1-x_{I1})^2\ \ (x_1-x_{I1})(x_2-x_{I2})\ \ (x_2-x_{I2})^2\ \ \ldots\ \ (x_2-x_{I2})^N], \tag{4}$$

*Project supported by the National Natural Science Foundation of China (Grant No. 11171208) and the Natural Science Foundation of Shanxi Province, China (Grant No. 2013011022-6).

†Corresponding author. E-mail: qyx819@163.com; 457612677@qq.com

© 2014 Chinese Physical Society and IOP Publishing Ltd

$$\boldsymbol{Q}(\boldsymbol{x}) = \sum_{I=1}^{N_\mathrm{p}} \bar{\Phi}_{\bar{a}_I}(\boldsymbol{x}-\boldsymbol{x}_I)\boldsymbol{H}(\boldsymbol{x}-\boldsymbol{x}_I)\boldsymbol{H}^\mathrm{T}(\boldsymbol{x}-\boldsymbol{x}_I), \quad (5)$$

$$\hat{H}(\boldsymbol{x}) = \sum_{I=1}^{N_\mathrm{p}} \hat{\Psi}_I(\boldsymbol{x})\boldsymbol{H}(\boldsymbol{x}-\boldsymbol{x}_I), \quad (6)$$

where N_p is the number of scatter particles in the compactly supported domain.

Suppose that the compactly supported domain is a rectangle whose center is $\boldsymbol{x}_I$, and its size is $2a_1 \times 2a_2$, and the weight function can be taken as the tensor product of the one-dimensional weight function

$$\Phi_a(\boldsymbol{x}-\boldsymbol{x}_I) = \frac{1}{a_1}\Phi\left(\frac{x_1-x_{I1}}{a_1}\right)\frac{1}{a_2}\Phi\left(\frac{x_2-x_{I2}}{a_2}\right). \quad (7)$$

In order to calculate the partial derivative of the shape function, equation (3) can also be written as

$$\bar{\Psi}_I(\boldsymbol{x}) = \boldsymbol{A}^\mathrm{T}(\boldsymbol{x})\boldsymbol{B}(\boldsymbol{x}), \quad (8)$$

where

$$\boldsymbol{A}^\mathrm{T}(\boldsymbol{x}) = \boldsymbol{H}^\mathrm{T}(\boldsymbol{x}-\boldsymbol{x}_I)\boldsymbol{Q}^{-1}(\boldsymbol{x}), \quad (9)$$

$$\boldsymbol{B}(\boldsymbol{x}) = [\boldsymbol{H}(0) - \hat{H}(\boldsymbol{x})]\bar{\Phi}_{\bar{a}_I}(\boldsymbol{x}-\boldsymbol{x}_I). \quad (10)$$

Because $\boldsymbol{Q}$ is symmetry, by solving Eq. (9), the partial derivative of $\boldsymbol{A}$ can be obtained

$$\boldsymbol{Q}(\boldsymbol{x})\boldsymbol{A}_{,i}(\boldsymbol{x}) = \boldsymbol{H}_{,i}(\boldsymbol{x}-\boldsymbol{x}_I) - \boldsymbol{Q}_{,i}(\boldsymbol{x})\boldsymbol{A}(\boldsymbol{x}), \quad (11)$$

so the partial derivative of shape function $\Psi_I(\boldsymbol{x})$ is

$$\bar{\Psi}_{I,i}(\boldsymbol{x}) = \boldsymbol{A}_{,i}^\mathrm{T}(\boldsymbol{x})\boldsymbol{B}(\boldsymbol{x}) + \boldsymbol{A}^\mathrm{T}(\boldsymbol{x})\boldsymbol{B}_{,i}(\boldsymbol{x}), \quad (i=1,2). \quad (12)$$

The interpolating RKPM shape function satisfies the property of the Kronecker delta function and the consistency condition.

The particle distribution on the 2D region $(x,y) \in [0,10] \times [0,10]$ is shown in Fig. 1. Here, 121 particles are arranged on it, and the three circle points stand for non-uniform particles and the three asterisk points stand for calculated points of the shape functions and their derived functions. For calculating them, the foundation primer is chosen as the basis function, and the cubic spline function is chosen as the weight function, and $a_1 = \alpha_1 d_\mathrm{c}$, $a_2 = \alpha_2 d_\mathrm{c}$, d_c is the smallest particle distance, and $\alpha_1 = 3.0$, $\alpha_2 = 0.49$. Figure 2 shows the shape of the interpolating RKPM function $\Psi_I(\boldsymbol{x})$. Figures 3 and 4 show the derived function figures of one particle. The figures demonstrate that the interpolating RKPM shape function has an excellent point interpolating characteristic and its derived function has a high order smoothness.

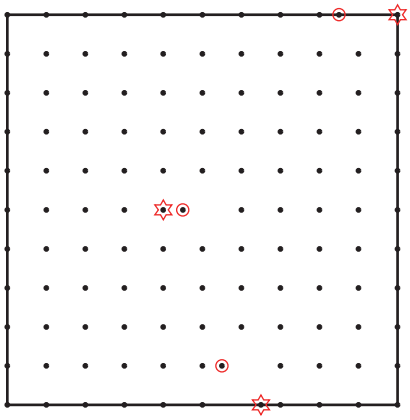


Fig. 1. (color online) Point distribution.

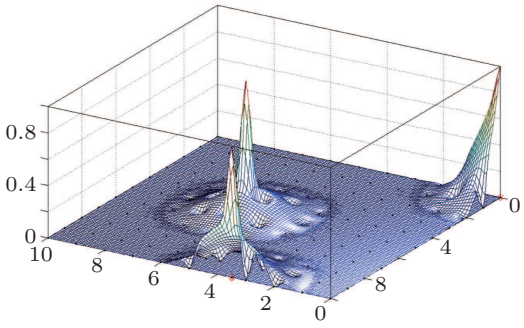


Fig. 2. (color online) The shape function of non-uniform particles.

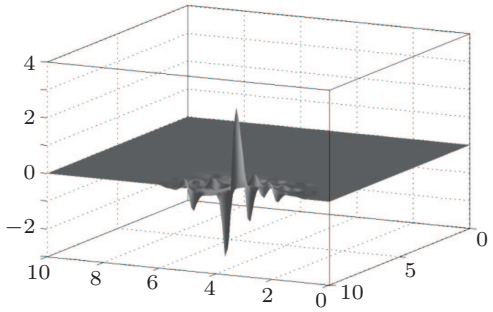


Fig. 3. The $\psi_{I,1}(\boldsymbol{x})$ at point $\boldsymbol{x}_{45}$.

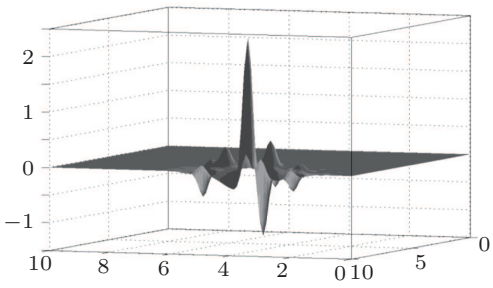


Fig. 4. (color online) The $\psi_{I,2}(\boldsymbol{x})$ at point $\boldsymbol{x}_{45}$.

3. Numerical examples

In this section, we will present some numerical examples to show the accuracy of the proposed interpolating RKPM

method. The algorithm of curve and surface fitting with the interpolating RKPM is as follows.

1) Arrange a series of particles in the question region, calculate their known function values.

2) Arrange a series of appraisement particles in the question region.

3) Circulate to every appraisement particle $\boldsymbol{x}$, ensure the number of particles and its shape function and derived function by the given compactly supported domain. Calculate the value of calculated point $\boldsymbol{x}$ in the compactly supported domain.

4) Solve the approximation value of $\boldsymbol{x}$ and fit curve or surface.

3.1. Curve fitting

Fit one-dimensional function

$$f(x) = \sin(x) + \cos(x), \quad x[0, 2\pi], \tag{13}$$

its differential coefficient is

$$f'(x) = \cos(x) - \sin(x), \quad x[0, 2\pi]. \tag{14}$$

Here, 21 scatter particles are uniformly employed on $[0, \pi]$, the function values of these particles are already known, 41 counted points are uniformly employed in the range. The basis function uses one-dimensional foundation primer $\boldsymbol{H}^{\mathrm{T}}(\boldsymbol{x} - \boldsymbol{x}_I) = [1, x - x_I]$. The weight function uses the one-dimensional cubic spline function. Figures 5 and 6 describe the function and the derived function which are obtained by the interpolating RKPM. Tables 1 and 2 give the function values of some points.

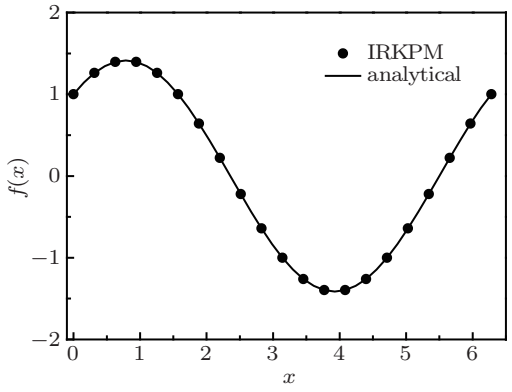


Fig. 5. Comparison of IPKPM shape function values and analytical solutions.

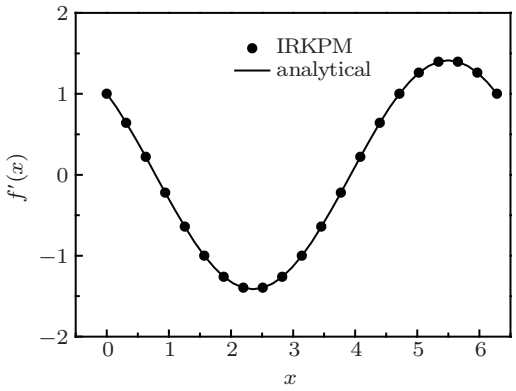


Fig. 6. Comparison of IPKPM derivative function values and analytical solutions.

Table 1. The values of the function at some points.

Abscissa	0	$\pi/5$	$2\pi/5$	$3\pi/5$	$4\pi/5$	π	$6\pi/5$	$7\pi/5$	$8\pi/5$	Maximal relative error
Analytical	1.00	1.40	1.26	0.64	–0.22	–1.00	–1.40	–1.26	–0.64	
IRKPM	1.00	1.39	1.25	0.64	–0.22	–1.00	–1.39	–1.25	–0.64	0.8%

Table 2. The values of the derived function at some points.

Abscissa	0	$\pi/5$	$2\pi/5$	$3\pi/5$	$4\pi/5$	π	$6\pi/5$	$7\pi/5$	$8\pi/5$	Maximal relative error
Analytical	1.00	0.22	–0.64	–1.26	–1.40	–1.00	–0.22	0.64	1.26	
IRKPM	1.00	0.22	–0.64	–1.25	–1.39	–1.00	–0.22	0.64	1.25	0.8%

It can be seen that the solutions of the interpolating RKPM agree well with the analytical solutions and that the interpolating RKPM has a good precision.

3.2. Surface fitting

A surface function can be express as

$$f(x,y) = \frac{\sin(\sqrt{x^2+y^2})}{\sqrt{x^2+y^2}}, \quad (x,y) \in [-8,8] \times [-8,8]. \tag{15}$$

Here, 33×33 particles and 66×66 appraisement points are employed on $[-8,8] \times [-8,8]$. The 2D foundation primer and the cubic spline weight function are employed. The exact values for the surface function are shown in Fig. 7. The result of the interpolating RKPM is shown in Fig. 8. Table 3 shows the specific values of some points. A good fitting is confirmed.

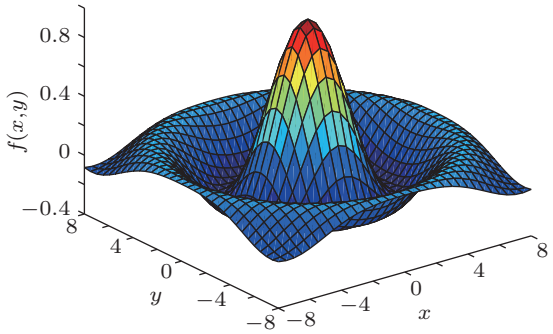


Fig. 7. (color online) Surface function $f(x,y)$.

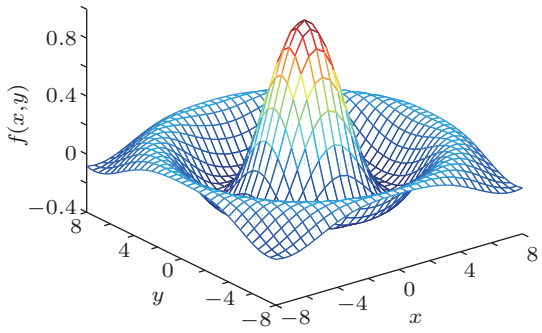


Fig. 8. (color online) Fitting of surface function $f(x,y)$.

Table 3. The values of the function at some points.

Coordinate	(–8, 0)	(–6, 0)	(–4, 0)	(–2, 0)	(0, 0)	(2, 4)	(3, 5)	Maximal relative error
Analytical	0.124	–0.047	–0.189	0.455	1.00	–0.217	–0.075	
IRKPM	0.123	–0.047	–0.188	0.452	1.00	–0.215	–0.075	0.9%

4. Conclusion

We deduce the derived function of the interpolating RKPM shape function, and show the high order smoothness of the approximation method. By using MATLAB programs and examples, the effectiveness of the interpolating RKPM for 2D problems is verified. This research shows that the interpolating RKPM has high precision characteristics. It can be concluded that the interpolating RKPM is an effective numerical method for engineering problems. In the fields of recognition technology and engineering mechanics analysis, the interpolating RKPM also has wide application prospects.

References

[1] Belytschko T, Lu Y Y and Gu L 1994 *Int. J. Numer. Meth. Eng.* **37** 229
[2] Cheng R J and Cheng Y M 2008 *Acta Phys. Sin.* **57** 6037 (in Chinese)
[3] Ren H P and Cheng Y M 2011 *Int. J.Appl. Mech.* **3** 735
[4] Aluru N R 2000 *Int. J. Number. Meth. Eng.* **47** 1083
[5] Cheng Y M and Li J H 2006 *Sci. China Ser. G: Phys. Mech. Astron.* **49** 46
[6] Chen L and Cheng Y M 2008 *Acta Phys. Sin.* **57** 1 (in Chinese)
[7] Chen L and Cheng Y M 2008 *Acta Phys. Sin.* **57** 6047 (in Chinese)
[8] Chen L and Cheng Y M 2010 *Sci. Sin. Phys. Mech. Astron.* **40** 242 (in Chinese)
[9] Chen L and Cheng Y M 2010 *Sci. China Phys. Mech. Astron.* **53** 954
[10] Chen L and Cheng Y M 2010 *Chin. Phys. B* **19** 090204
[11] Cheng Y M and Li J H 2005 *Acta Phys. Sin.* **45** 548 (in Chinese)
[12] Cheng Y M, Li R X and Peng M J 2012 *Chin. Phys. B* **21** 090205
[13] Wang J F and Cheng Y M 2013 *Chin. Phys. B* **22** 030208
[14] Cheng Y M and Chen M J 2003 *Acta Mech. Sin.* **35** 181 (in Chinese)
[15] Peng M J and Cheng Y M 2009 *Eng. Anal. Bound. Elem.* **33** 77
[16] Ren H P, Cheng Y M and Zhang W 2009 *Chin. Phys. B* **18** 4065
[17] Ren H P, Cheng Y M and Zhang W 2010 *Sci. China Ser. G: Phys. Mech. Astron.* **53** 758
[18] Qin Y X and Cheng Y M 2009 *Chinese Journal of Theoretical and Applied Mechanics* **41** 898 (in Chinese)
[19] Cheng Y M, Liew K M and Kitipornchai S 2009 *Int. J. Numer. Meth. Eng.* **78** 1258
[20] Liu W K, Chen Y and Uras R A 1996 *Comput. Meth. Appl. Mech. Eng.* **139** 91
[21] Li S and Liu W K 1997 *Comput. Meth. Appl. Mech. Eng.* **143** 113
[22] Chen J S, Yoon S, Wang H P and Liu W K 2000 *Comput. Meth. Appl. Mech. Eng.* **181** 117
[23] Cheng Y M and Peng M J 2005 *Sci. China Ser. G: Phys. Mech. Astron.* **48** 641
[24] Cheng Y M, Wang J F and Bai F N 2012 *Chin. Phys. B* **21** 090203
[25] Wang J F and Cheng Y M 2012 *Chin. Phys. B* **21** 090203
[26] Cheng Y M, Wang J F and Li R X 2012 *Int. J. Appl. Mech.* **4** 1250042